Delivery of nitric oxide-releasing silica nanoparticles for *in vivo* revascularization and functional recovery after acute peripheral nerve crush injury

https://doi.org/10.4103/1673-5374.335160

Date of submission: March 19, 2021

Date of decision: April 18, 2021

Date of acceptance: May 11, 2021

Date of web publication: February 8, 2022

Jung Il Lee[1, #], Ji Hun Park[1, #], Yeong-Rim Kim[2], Kihak Gwon[2], Hae Won Hwang[3, 4], Gayoung Jung[3], Joo-Yup Lee[5], Jeong-Yun Sun[4], Jong Woong Park[1, *], Jae Ho Shin[2, 6, *], Myoung-Ryul Ok[3, *]

From the Contents

Graphical Abstract *Injection of nitric oxide-releasing silica nanoparticles (NO-SNs) mixed with fibrin gel enhances revascularization and accelerates the process of peripheral nerve regeneration and functional recovery in rats after sciatic nerve injury*

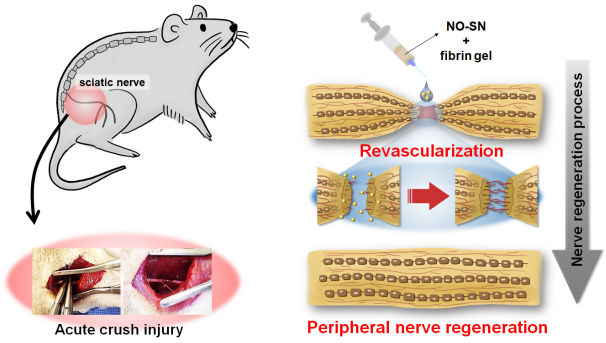

Abstract

Nitric oxide (NO) has been shown to promote revascularization and nerve regeneration after peripheral nerve injury. However, *in vivo* application of NO remains challenging due to the lack of stable carrier materials capable of storing large amounts of NO molecules and releasing them on a clinically meaningful time scale. Recently, a silica nanoparticle system capable of reversible NO storage and release at a controlled and sustained rate was introduced. In this study, NO-releasing silica nanoparticles (NO-SNs) were delivered to the peripheral nerves in rats after acute crush injury, mixed with natural hydrogel, to ensure the effective application of NO to the lesion. Microangiography using a polymer dye and immunohistochemical staining for the detection of CD34 (a marker for revascularization) results showed that NO-releasing silica nanoparticles increased revascularization at the crush site of the sciatic nerve. The sciatic functional index revealed that there was a significant improvement in sciatic nerve function in NO-treated animals. Histological and anatomical analyses showed that the number of myelinated axons in the crushed sciatic nerve and wet muscle weight excised from NO-treated rats were increased. Moreover, muscle function recovery was improved in rats treated with NO-SNs. Taken together, our results suggest that NO delivered to the injured sciatic nerve triggers enhanced revascularization at the lesion in the early phase after crushing injury, thereby promoting axonal regeneration and improving functional recovery.

Key Words: crush injury; nerve injury, nerve regeneration; nitric oxide; peripheral nerve; revascularization; silica nanoparticles

Introduction

Peripheral nerve injury (PNI) is primarily caused by motor vehicle accidents, industrial accidents, stretching or crushing after falls, stab or laceration injuries, gunshot injury, and fractures (Tapp et al., 2019). PNI results in functional impairment or permanent disability and is associated with substantial social and personal costs to the affected individual (Tapp et al., 2019; Bergmeister et al., 2020). As axonal regeneration and growth support of Schwann cells diminishes with increasing time after an injury and distance from the injured site, it is a race against time for regenerating axons to regain satisfactory function (Chan et al., 2014). Thus, the acceleration of axonal regeneration may allow partial or complete functional recovery after PNI.

Manipulation of the nitric oxide (NO) supply in the neural

[1]Department of Orthopedic Surgery, College of Medicine, Korea University, Seoul, Republic of Korea; [2]Medical Sensor Biomaterial Research Institute, Kwangwoon University, Seoul, Republic of Korea; [3]Center for Biomaterials, Korea Institute of Science & Technology, Seoul, Republic of Korea; [4]Department of Materials Science and Engineering, Seoul National University, Seoul, Republic of Korea; [5]Department of Orthopedic Surgery, College of Medicine, Catholic University, Seoul, Republic of Korea; [6]Department of Chemistry, Kwangwoon University, Seoul, Republic of Korea

*Correspondence to: Jong Woong Park, MD, PhD, ospark@korea.ac.kr; Jae Ho Shin, PhD, jhshin@kw.ac.kr; Myoung-Ryul Ok, PhD, omr2da@kist.re.kr.
https://orcid.org/0000-0003-2751-2519 (Jong Woong Park); https://orcid.org/0000-0002-6117-6910 (Jae Ho Shin);
https://orcid.org/0000-0003-2733-9074 (Myoung-Ryul Ok)
#These authors contributed equally to this work.

Funding: *This work was supported by the National Research Foundation of Korea (NRF), funded by the Ministry of Science and ICT, Nos. NRF-2015R1C1A1A02036830 (to JIL) and NRF-2015M3A9E2029186 (to JHS). This work was also supported by a grant of the Korea Institute of Science and Technology, Nos. 2V05460/2V08630 (KIST-KU TRC program), 2E31121 (to MRO) and a grant of Korea University Anam Hospital (to JHP and JWP).*

How to cite this article: *Lee JI, Park JH, Kim YR, Gwon K, Hwang HW, Jung G, Lee JY, Sun JY, Park JW, Shin JH, Ok MR (2022) Delivery of nitric oxide-releasing silica nanoparticles for in vivo revascularization and functional recovery after acute peripheral nerve crush injury. Neural Regen Res 17(9):2043-2049.*

regenerative process is one possible way to boost axonal regeneration after PNI. NO is a crucial bioregulatory molecule in degenerative and regenerative processes of peripheral nerves after PNI, for example, in Wallerian degeneration (Kelihoff et al., 2002a), vascular remodeling in angiogenesis (Kelihoff et al., 2002b), and re-establishment of neuromuscular junctions (Kelihoff et al., 2002b; Moreno-Lopez, 2010). During neural regeneration, the NO supply depends on three major types of nitric oxide synthase (NOS) isoforms: constitutive neuronal (nNOS), endothelial (eNOS), and inducible (iNOS) forms (Gonzalez-Hernandez and Rustioni, 1999a; Moreno-Lopez, 2010). NO produced by eNOS in the peripheral nerves enhances revascularization, hyperemia, and dilation of blood vessels, helping to remove cell debris by activating the infiltration of inflammatory cells (Kelihoff et al., 2002a, b) and recruitment of other cells necessary for regeneration from the bloodstream (Gonzalez-Hernandez and Rustioni, 1999a; Kelihoff et al., 2002b; Moreno-Lopez, 2010). NO originating from the upregulation of nNOS/iNOS plays a critical role in Wallerian degeneration and axon regeneration (Levy et al., 2001; Kelihoff et al., 2002a; Zochodne and Levy, 2005).

Despite its important biological roles, NO has not been widely used as a therapeutic material in PNI because of the lack of suitable vehicles to facilitate storage and controlled and prolonged delivery. The silica nanoparticle system has been reported to chemically store NO molecules (up to 1780 nmol/mg) and spontaneously release them at physiological temperature and pH under aqueous conditions over a clinically significant time scale (up to 30 hours) (Shin et al., 2007; Shin and Schoenfisch, 2008). Previous studies have shown the anti-microbial and anti-tumor effects of NO-releasing silica nanoparticles (NO-SNs) (Hetrick et al., 2008, 2009; Stevens et al., 2010). However, as nerve regeneration involves a complex series of biological steps, it is essential to determine a suitable carrier material to enable NO supply only to the lesion, to prevent negative effects on the surrounding tissue.

Herein, we describe a novel method for the application of NO-SNs in PNI in male rats (we used male mice to avoid the potential influence of the hormonal status or estrous cycles on regeneration in female mice. In addition, because traumatic peripheral nerve injury mostly occurs in male patients, translational research of nerve regeneration is usually performed with male animals), which involves mixing nanoparticles with a biocompatible natural hydrogel. Inspired by the controllable gelation behavior and biocompatibility of fibrin (Noori et al., 2017), this material was chosen as a carrier for NO-SNs so that the nanoparticles embedded in the glue-like fibrin gel may adhere to the damaged sciatic nerve of rats and release NO only at the site of injury. Histological analyses were performed to reveal revascularization and growth of myelinated axons. Furthermore, the physical performance of animals was recorded, because the ultimate aim of peripheral nerve regeneration is the recovery of functional performance, which is sufficient for the social comeback of the individual.

Materials and Methods

Synthesis of NO-SNs

The NO-SNs were synthesized and characterized as described previously (Shin and Schoenfisch, 2008; Hetrick et al., 2009). Briefly, an aminoalkoxysilane solution was prepared by dissolving 6.8 mM N-methylaminopropyltrimethoxysilane (MAP3; Gelest, Tullytown, PA, USA) in a mixture of 16 mL ethanol (EtOH) and 4 mL methanol (MeOH), in the presence of 6.8 mM sodium methoxide ($NaOCH_3$; Fluka, Buchs, Switzerland). The solution was then placed in 10-mL vials equipped with stir bars. The vials were placed in a Parr bottle, connected to an in-house NO reactor, and flushed with argon six times to remove O_2 from the solution. The reaction bottle was pressurized to 10 atm (1.013 MPa) NO for 3 days with continuous stirring of the silane solution. Before removing the N-diazeniumdiolate-modified silane sample (MAP3/NO), unreacted NO was purged from the chamber with Ar. The silane solution was prepared by mixing 2.8 mM tetraethoxysilane (TEOS; Fluka, Buchs, Switzerland) and MAP3/NO (6.5 mM; corresponding to 70 mol%, balance TEOS) in the EtOH/MeOH solution for 2 minutes. The silane solution was then added to EtOH (22 mL) with an ammonia catalyst (6 mL, 30% (w/w) in water), and mixed vigorously for 30 minutes at 4°C. The precipitated nanoparticles were collected by centrifugation (2516 × *g*, 5 minutes), washed with EtOH several times, dried under ambient conditions for 1 hour, and stored in a sealed container at –20°C until use.

NO release kinetics of MAP3/NO nanoparticles was monitored in deoxygenated phosphate-buffered saline (PBS; 0.01 M, pH 7.4) at 37°C using a Sievers NOA 280i Chemiluminescence Nitric Oxide analyzer (Sievers Instruments, Boulder, CO, USA) (Shin et al., 2007; Shin and Schoenfisch, 2008). The instrument was calibrated with air passed through a zero filter (0 ppm (0.0001%) NO) and 45 ppm of NO standard gas (balance N_2). The morphology and size of the NO-SNs were analyzed using scanning electron microscopy.

Ethics statement

All animal experiments were conducted according to the protocol approved by the Institutional Animal Care and Use Committee of the Korea University College of Medicine (IACUC Approval No. 2016-0266) on November 30, 2017. This study was reported in accordance with the ARRIVE 2.0 guidelines (Animal Research: Reporting of *In Vivo* Experiments) (Percie du Sert et al., 2020).

Surgical procedure

Fifty-four male Lewis rats weighing 250–300 g were randomly divided into two groups of 27 each and received a standardized sciatic nerve crushing injury, as described in **Figure 1**. The rats were anesthetized using isoflurane inhalation; animals were sedated with 5% isoflurane in a plastic chamber and then moved on to the surgical field for a survival procedure maintained under 3% isoflurane administered via a mask placed over the mouth. The right limb and buttock were shaved, washed with 70% ethanol, and prepared with povidone iodine. The sciatic nerve was carefully exposed around the trifurcation site using gluteal splitting. All rats received sciatic nerve crushing injury (6 mm in length) on a site just proximal to the trifurcation, made by closing a new smooth-tipped needle holder (Integra Miltex, Plainsboro, NJ, USA) to the third notch for 20 seconds (Sundem et al., 2016). Fibrin gel, a natural hydrogel, was subsequently applied around the crushed nerve, with and without NO-SNs. Only fibrin gel without NO-SNs was injected into animals of the control group: 1 µL of thrombin (T4648, Sigma-Aldrich, St. Louis, MO, USA; 50 U/mL in sterile water) was diluted with 37.5 µL of phosphate-buffered saline (PBS), and then, 12.5 µL of filtered fibrinogen solution (F8630, Sigma-Aldrich; 10 mg/mL in DPBS with Ca^{2+} and Mg^{2+}) was added to the PBS-diluted thrombin solution just before the application of the gel to prevent pre-clotting. For the treatment of animals in the NO-treated group, NO-SNs were dissolved in PBS at a concentration 4/3-fold higher than the target concentration, and 37.5 µL of this solution was homogeneously mixed with 1 µL of thrombin. The same amount (12.5 µL, without NO-SNs) and concentration of fibrinogen solution as used in the control group was added to the mixture of thrombin and NO-SNs. The final concentration of NO in the fibrin gel was 70 µM. After confirmation of clotting of the fibrin gel around the crush site, the skin was sutured with 4-0 Prolene, which was removed 14 days after surgery. All rats received a single intramuscular injection of ketoprofen (5 mg/kg) for immediate postoperative pain control and enrofloxacin (5 mg/kg) to prevent postoperative infection. After the surgery procedures, rats were returned to their cages and raised in an environment with a 12-hour light/dark cycle and provided with food and water *ad libitum*.

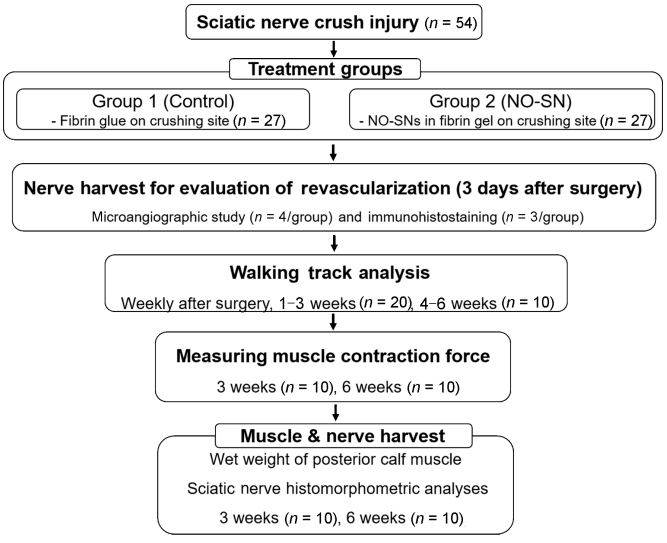

Figure 1 | **Flowchart describing the experimental procedures and animal assignment.**
NO-SN: Nitric oxide-releasing silica nanoparticle.

Microangiography

The effect of NO delivery on revascularization at the crushed nerve was analyzed using microangiography and immunohistochemical staining of nerves. We performed microangiography (Giusti et al., 2016) to evaluate revascularization around the crush site of the nerve 3 days after nerve crush. After rats were anesthetized with an intravenous injection of alfaxalone (1–1.5 mg) into the ventral tail vein, the rib cage was carefully opened to expose the heart, and a cannula was inserted into the aorta through a small incision in the left ventricle. A small incision was made in the right atrium for drainage, and the region was flushed with saline mixed with heparin until the liver turned pale. This was followed by flushing with 200 mL of 4% paraformaldehyde. Blue-colored microangiographic polymer dye (Microfil®, Flowtech, Carver, MA, USA) (40 mL) was injected through the cannula under physiological pressure (100 mmHg) using an infusion pump (Harvard Apparatus, Holliston, MA, USA). The specimen was stored overnight at 4°C for complete polymerization of the injected polymer dye. Sciatic nerve segments, including those from the crushing site, were harvested and processed through an alcohol-methyl salicylate clearing sequence to clarify the vessels. An image of the processed nerve segments was captured to analyze the degree of vascular density using ImageJ software ver 1.51 (National Institutes of Health, Bethesda, MD, USA). Vascular density was determined by the portion of the area occupied by the blue-colored vessels at the crushing site of the sciatic nerve.

Determination of sciatic functional index by walking track analysis

Improvements in sciatic nerve function were evaluated based on the sciatic functional index (SFI) determined by walking track analysis. Walking track analysis was performed weekly to evaluate the motor function recovery as described previously (Bain et al., 1989). We selected two footprints per limb for measurements, based on the clarity and morphology of the paw and anatomic structures. The third toe to heel (print length, PL), the first to fifth toe (toe spread, TS), and the second to fourth toes (intermediate toe spread, IT) lengths were measured. The SFI was calculated using the following formula described by Bain et al. (1989):

$$SFI = -(38.3 \times (IPL-NPL))/NPL + (109.5 \times (ITS-NTS))/NTS + (13.3 \times (IIT-NIT))/NIT - 8.8$$

where "I" and "N" denote "injured" and "normal," respectively.

In general, an index of 0 indicates the normal function, and an index of -100 represents a complete loss of function. Because 10 animals in each group were sacrificed at 3 weeks, SFI data were obtained from 20 animals in each group at 3 weeks and for 10 animals at 6 weeks.

Maximum isometric tetanic force and wet muscle weight

The isometric tetanic force of the tibialis anterior (TA) was measured to evaluate the effect of NO treatment on muscle function recovery. The contraction force values are presented as percentages on the contralateral side. To assess muscle function recovery, at 3 and 6 weeks after nerve crush the maximum isometric tetanic force was determined as described previously (Lee et al., 2013). Briefly, rats were anesthetized as described earlier, and the TA tendon insertion site was exposed and released from the extensor retinaculum. The mid-portion of the TA muscle remained under the skin to prevent cooling and desiccation. The hind limb was stabilized with two Kirschner wires placed at the distal femur and distal tibia. The exposed TA tendon was tied with black silk, the other end of which was connected to an isometric force transducer (Harvard Apparatus, Holliston, MA, USA). The anchoring black silk was positioned such that the TA muscle was placed in a position similar to its anatomical position. The force transducer signal was processed using LabScribe software (iWorx system, Dover, NH, USA). Two custom-made small hook-shaped bipolar stimulating electrodes were placed using a CK-100 field stimulator (CB Science) on the sciatic nerve proximal to the crush site. All stimulating pulses were of the same settings as in our previous study (Lee et al., 2013) for all measurements: preload, 10 g; stimulus intensity, 10 V; pulse duration, 2 ms; and pulse frequency, 100 Hz. Stimulations were applied five times, and the TA muscle was rested for 2 minutes between stimulations, with no preload to avoid muscle fatigue. The maximum isometric tetanic force was determined to be the highest force. The same procedure was performed on the contralateral side. After the TA muscle contraction procedure, we harvested the posterior calf muscle (gastrocnemius and soleus) from the surrounding tissues and recorded the weight in grams. The TA muscle contraction force and posterior calf muscle weight were recorded as percentages of the contralateral side.

Histomorphometry analysis

The sciatic nerves were harvested at 3 days and 3 and 6 weeks after nerve crush. All nerves were fixed with 4% paraformaldehyde. The nerves harvested on day 3 after injury were embedded in paraffin, and 5-µm cross-sections were taken from the crush site. Immunohistochemical staining was performed using primary antibody goat anti-rat CD34 (AF4117, R&D system, Minneapolis, MN, USA, 1:100, AB_2074613) overnight at 4°C. Sections were washed with PBS and then incubated with rabbit anti-goat IgG (AI-5000, Vector Laboratories, Burlingame, CA, USA, 1:100, AB_2336125) for 1 hour at 37°C. Staining for CD34, a transmembrane protein in the endothelial cells of blood vessels, was used to evaluate the number of regenerated vessels at the crush site. The number of vessels, which are shown as brown-colored cells lining the luminal structure, was counted manually using a light microscope (BX46, Olympus, Tokyo, Japan) in the whole nerve section at a magnification of 200×.

For quantitative analysis of the myelinated axons, the N ratio, myelin thickness, and G-ratio, harvested nerves at 3 or 6 weeks after the injury were stained with toluidine blue. The nerves harvested at 3 or 6 weeks after injury were embedded in epoxy resin, cut into 1-µm sections, 2 mm distal to the crush site, and stained with toluidine blue (89640, Sigma-Aldrich). The image of the cross-sectioned tibial division of the sciatic nerve at the digital level of the crushing site was captured at 200× magnification, using a charge-coupled device camera (DP21, Olympus, Tokyo, Japan) attached to a light microscope (BX46, Olympus). The images were analyzed for the area in a semiautomatic fashion using ImageJ to determine the number of myelinated axons and the N ratio, which was calculated as the total myelinated axon area divided by the total nerve area (Tobin et al., 2014; Lee et al., 2016). Myelin thickness and G-ratio, which were calculated as axonal diameter divided by axoglial diameter, were measured using 30 randomly selected axons in each image (300 axons were analyzed per group).

Statistical analysis

All results are expressed as mean ± standard error of the mean (SEM). Mann-Whitney *U* test was used to detect statistical differences between two groups of vascular density and the number of vessels. One microangiographic specimen in the control group was excluded from the analysis because the specimen was improperly stained. Multiple unpaired *t*-test was used to detect statistical differences between two groups of SFI, muscle contraction force, muscle weight, and histologic analysis of nerve. Analysis of variance was used to detect statistical improvements in the SFI with time. Statistical analysis was performed using GraphPad Prism 9 (GraphPad Software, San Diego, CA, USA). Differences were considered significant at P-values < 0.05. A power analysis was performed based on the differences in SFI found between groups in previous publications (Elfar et al., 2008). Based on 35% difference detection and the desired power level of > 80%, we determined that a sample size of minimum five mice per group for functional outcomes. Previous works (Geary et al., 2017; Lee et al., 2020) had suggested that a group size of 3 or 4 would be sufficient for immunohistochemical studies. Biochemical and histological analyses were conducted blinded to the treatment, whereas *in vivo* microscopy and analysis were not performed blinded to the conditions of the experiments.

Results

Nitric oxide release from silica nanoparticles

The total amount of NO (t[NO]) released from MAP3/NO nanoparticles was approximately 6.8 µM/mg, with a maximum NO flux ([NO]m) of 155,000 ppb/mg and a NO release half-life (t1/2) of 5 minutes. The diameter of MAP3/NO nanoparticles analyzed using scanning electron microscopy was approximately 120 nm (**Figure 2**), similar to the previously reported value (Shin et al., 2007).

Revascularization

The results of microangiography are presented in **Figure 3**. Based on microangiography evaluation, the regenerated endoneurial vessels passing through the crushing injury site were identified in specimens from all animals, except in one control specimen which was improperly stained and thus excluded from the analysis. Relative to the control group, more vessels stained with blue dye were found in the NO-treated nerves. The vascular density at the crushing site of the sciatic nerve was significantly greater in the NO-treated group than in the control group (P < 0.05).

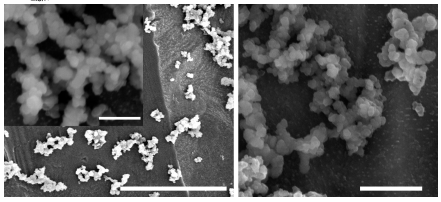

Figure 2 | **Scanning electron microscopy images of the aggregated nitric oxide-releasing silica nanoparticles (bright) on the carbon tape (dark).**
The diameter of the nanoparticles is about 120 nm. The scale bars on the left, left-inset, and right represent 5 μm, 500 nm, and 1 μm, respectively.

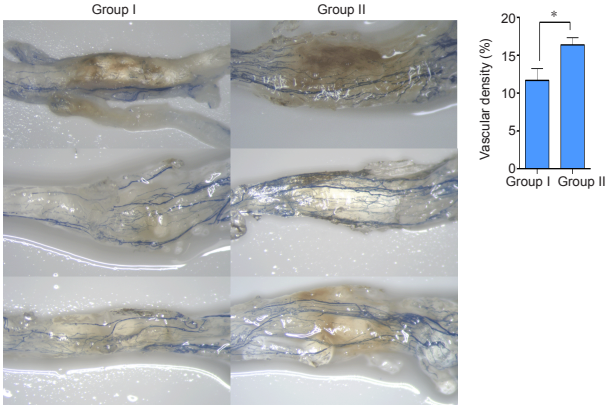

Figure 3 | **The level of revascularization after treatment with NO-SNs.**
Microangiography was performed using a blue-colored polymer dye on day 3 after nerve crush injury to evaluate the level of revascularization after treatment with NO-SNs. The swollen and yellowish-colored area is the crush site of the sciatic nerve in the animal. There were more blue colored capillaries in the crush site in animals treated with NO-SNs (NO) compared with the control group (without NO-SNs), which suggest that the NO-SNs (MAP3/NO) promoted vascular proliferation in the crush site of rat sciatic nerve (n = 3/group); *P < 0.05 (Mann-Whitney U test). Data are expressed as the mean ± SEM. Group I: Crushed nerve; Group II: crushed nerve treated with NO-SNs). NO-SNs: Nitric oxide-releasing silica nanoparticles.

For direct identification of the newly formed vessels, immunohistochemical staining was performed targeting CD34, a marker for evaluating angiogenesis (**Figure 4**). The number of vessels stained with CD34 at the nerve sections in the control group is similar to the NO-treated group (P = 0.38).

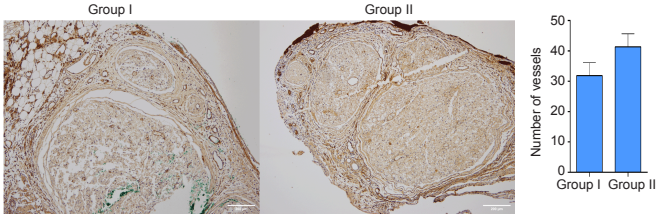

Figure 4 | **Revascularization after treatment with NO-SNs.**
On day 3 after nerve crush injury, an increase in the number of CD34 stained blood vessels, shown as brown-colored cells lining the luminal structure, was observed in representative immunohistochemistry images (200×) of nerve treated in rats treated with NO-SNs (NO). Scale bars: 200 μm. There was no significant difference in the number of vessels (/whole cross-sectioned nerve) stained with CD34 between the two groups (n = 3/group; P = 0.13). Data are expressed as the mean ± SEM. Group I: Crushed nerve/control; Group II: crushed nerve treated with NO-SNs. NO-SNs: Nitric oxide-releasing silica nanoparticles.

Motor function of rat hind limbs

The SFI for animals in the control group improved from 2 weeks to 5 weeks after injury (from 2 weeks to 4 weeks after injury, P < 0.0001; from 4 weeks to 5 weeks after injury, P < 0.01) and the SFI for animals in the NO-treated group improved from 2 weeks to 4 weeks after injury (P < 0.0001). From 2 weeks to 4 weeks after injury, the SFI of animals in the NO-treated group exhibited a significant functional improvement compared to that in the animals of the control group (P < 0.05; **Figure 5C**). In summary, after crush injury, NO-SN treatment accelerated both revascularizations (3 days after injury, P < 0.01, **Figure 3**) and recovery of sciatic nerve function (from 2 weeks to 4 weeks after injury, P < 0.05; **Figure 5**). However, the SFIs of the NO-treated and control groups were identical at 5 weeks after injury (**Figure 5C**).

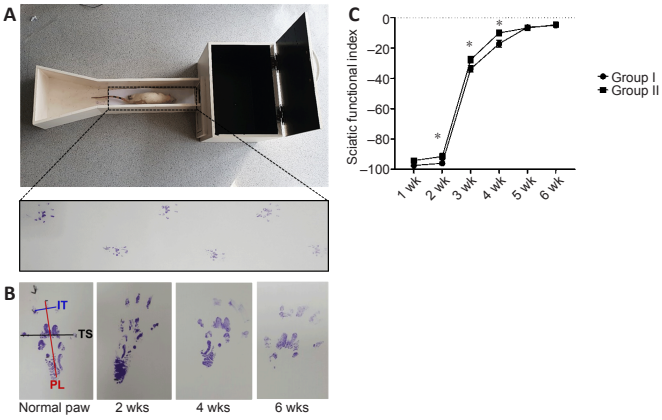

Figure 5 | **Walking track analysis for the calculation of the SFI.**
(A) Custom-made corridor for rats to walk straight. A dark cage was installed on the opposite side to guide the rat walk in the front direction. (B) Representative photographs of the footprint of a rat after crushing injury of sciatic nerve showing parameters for the calculation of the SFI. Compared with a normal paw, the injured side shows decreased intermediate toe spread (IT, blue) and toe spread (TS, black) and increased paw length (PL, red) at 2 weeks. Serial measurements at 4 and 6 weeks show gradual improvements, proving the recovery of motor function. (C) The SFI for animals in both groups improved from 2 weeks to 5 weeks after injury. Based on the SFI change, NO-SNs promoted functional recovery until 4 weeks after nerve crush injury. Improvements in sciatic function in group II was faster than in group I by 4 weeks of injury. n = 20/group (1–3 weeks) and 10/group (4–6 weeks). Data are expressed as the mean ± SEM. *P < 0.05 (multiple unpaired t-test). Group I: Crushed nerve/control; Group II: crushed nerve treated with NO-SNs. NO-SNs: Nitric oxide-releasing silica nanoparticles; SFI: sciatic functional index.

Muscle function and muscle atrophy

As presented in **Figure 6**, NO-SNs enhanced the isometric tetanic muscle force of the TA at 3 and 6 weeks after injury, and a significant effect of NO-SNs was apparent, with a mean intergroup difference at 6 weeks after injury (P < 0.05).

The wet weight of calf muscle (gastrocnemius and soleus) in animals of the NO-treated group was higher compared with that in the control group at 3 and 6 weeks after injury. However, a statistically significant difference between the two groups was observed only at 3 weeks (P < 0.05), but not at 6 weeks (P = 0.1; **Figure 7**) after injury.

Nerve regeneration

The number of myelinated axons and the N ratio increased over time in both groups (**Figure 8B** and **C**). The number of myelinated axons was significantly higher in animals treated with NO-SNs compared with the untreated animals 3 weeks after injury (P < 0.05; **Figure 8B**). However, this intergroup difference was not significant at 6 weeks after injury. The N ratio was higher in animals treated with NO-SNs compared with the untreated animals at 3 and 6 weeks after injury, but there was no significant difference between the two groups (**Figure 8C**). NO-SNs treated animals had significantly thicker myelin at 3 and 6 weeks after injury (P < 0.01; **Figure 8D**) and significantly lower G-ratio at 3 weeks after injury compared with the untreated animals (P < 0.0001; **Figure 8E**).

Discussion

Our results demonstrate that NO-SNs (MAP3/NO) enhance revascularization and nerve regeneration, and improve the motor function in a rat model of sciatic nerve injury.

NO is a pivotal neuromediator in revascularization of peripheral nerves and vasodilation for cell recruitment after PNI (Keilhoff et al., 2002b; Zochodne et al., 2005). Endogenous NO levels increase as soon as 2 days after PNI, and are modulated by eNOS overexpression in the vasa nervosum of the distal stump (Gonzalez-Hernandez and Rustioni, 1999a). Endogenous NO generated by eNOS plays a

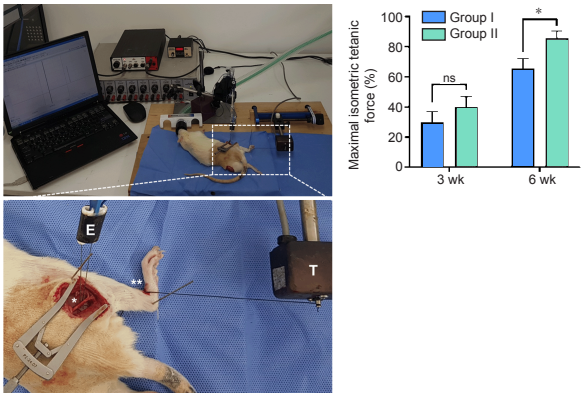

Figure 6 | NO-SNs enhance muscle contraction force reduced by asciatic nerve crush injury.

Left: Experimental setup for measurement of the maximum isometric tetanic force. After visualization of the sciatic nerve (*), the hind limb was stabilized by two Kirschner wires placed at the distal femur and distal tibia. The tibialis anterior (TA) tendon insertion site was released from the extensor retinaculum, while the mid-portion of the muscle remained under the skin to prevent cooling and desiccation. The exposed TA tendon (**) was connected with an isometric force transducer (T) using black silk. A custom-made bipolar hook electrode (E) was placed on the sciatic nerve proximal to the crush site. The force transducer signal was processed on a personal computer using dedicated software. **Right:** NO-SNs improved the isometric tetanic force of tibialis anterior (TA) at 6 weeks after nerve crush injury significantly. The values of the contraction forces are presented as percentages of the contralateral side. The isometric tetanic force of TA in group II was greater than in group I at 3 and 6 weeks after injury. The statistically significant difference between the two groups was observed at only 6 weeks after injury (n = 10/group; *P < 0.05 (multiple unpaired t-test). Group I: Crushed nerve; Group II: crushed nerve treated with NO-SNs. Data are expressed as the mean ± SEM. NO-SNs: Nitric oxide-releasing silica nanoparticles; ns: not significant.

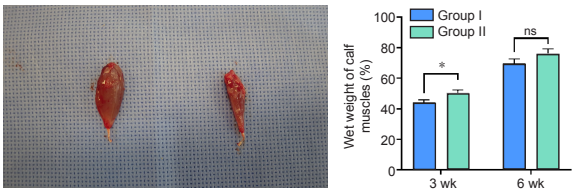

Figure 7 | NO-SNs prevent denervation-induced muscle atrophy.

The values of the muscle weight are presented as percentages of the contralateral side (left, contralateral calf muscle; right, atrophied muscle by crush injury). The wet weight of calf muscle (gastrocnemius and soleus) in group II was higher than in group I at 3 and 6 weeks of injury. Statistically significant differences between the two groups were observed at 3 weeks (n = 10/group; *P < 0.05 (multiple unpaired t-test), but not significant at 6 weeks (n = 10/group; P = 0.1) after injury. Data are expressed as the mean ± SEM. Group I: Crushed nerve/control; Group II: crushed nerve treated with NO-SNs. NO-SNs: Nitric oxide-releasing silica nanoparticles; ns: not significant.

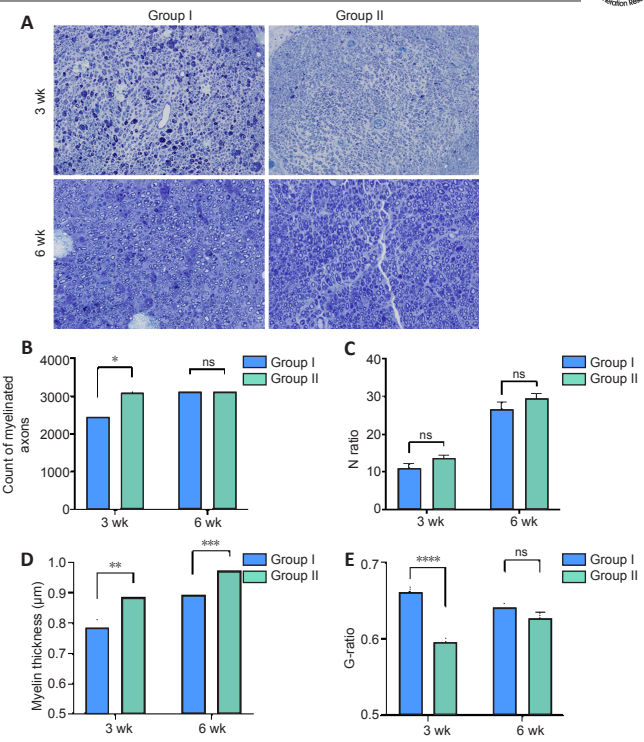

Figure 8 | NO-SNs promote the regeneration of myelinated axons and myelin repair.

(A) Representative images showing the histology of cross-sections of a sciatic nerve stained with toluidine blue. Scale bars: 50µm. (B) NO-SNs enhance nerve regeneration after nerve crush injury. The number of myelinated axons in animals of group II was significantly higher than those in group I at 3 weeks after injury (n = 6/group; *P < 0.05). (C) N ratio, which was calculated as the total myelinated axon area divided by the total nerve area, in group II was higher than in group I. However, this difference was not statistically significant (n = 6/group; week 3, P = 0.1; week 6, P = 0.2). (D) The myelin thickness in group II was significantly higher than in group I at 3 and 6 weeks after injury. (n = 10/group; **P < 0.01, ***P < 0.001). (E) G-ratio (axonal diameter/axoglial diameter) in group II animals was higher than in group I at 3 and 6 weeks after injury. However, this difference was statistically significant only at 3 weeks after injury. (n = 10/group; ****P < 0.0001 (multiple unpaired t-test). Data are expressed as the mean ± SEM. Group I: Crushed nerve/control; Group II: crushed nerve treated with NO-SNs. NO-SNs: Nitric oxide-releasing silica nanoparticles; ns: not significant.

critical role in revascularization, remodeling of vessels, hyperemia, vasodilation, and inflammatory cell infiltration (Rudic et al., 1998; Gonzalez-Hernandez and Rustioni, 1999a; Kelihoff et al., 2002b). A 2-day delay in revascularization was observed in eNOS knockout (KO) mice relative to wild-type mice after nerve transection and autogenous nerve grafting (Kelihoff et al., 2002b). NO-mediated vasodilation helps to remove cell debris, recruit inflammatory cells, such as macrophages from the bloodstream, and support the metabolic processes for regenerating axons and other cellular elements (Kelihoff et al., 2002a; Moreno-Lopez, 2010).

NO promotes revascularization following PNI, but also plays a critical role in Wallerian degeneration, axonal regrowth, and functional recovery after PNI (Gonzalez-Hernandez and Rustioni, 1999a, b; Kelihoff et al., 2002a; Kikuchi et al., 2018). Functional recovery is impaired after nerve transection and repair in nNOS KO mice because of delayed Wallerian degeneration, increased uncontrolled axonal sprouting, and delayed nerve regeneration (Kelihoff et al., 2002a). nNOS is a major factor in axonal sprouting and synaptogenesis in nNOS KO mice compared with wild-type mice after nerve transection (Gonzalez-Hernandez and Rustioni, 1999a, b). Levy et al. (2001) made similar observations about Wallerian degeneration, axonal regrowth, and functional recovery in iNOS KO mice. Thus, the lack of NO-mediated stimulation in nNOS or iNOS KO mice might lead to delayed structural changes in nerves and functional recovery. Keilhoff et al. suggested that manipulation of the NO supply might offer therapeutic options for the treatment of PNI (Kelihoff et al., 2002a).

In this context, it is worth noting that in the present study, locally delivered exogenous NO supply might enhance the revascularization process and functional recovery in the case of PNI. Functional recovery following traumatic or iatrogenic peripheral nerve injury is unpredictable. These injuries require many complex microsurgical procedures, such as neurorrhaphy, nerve grafting, and nerve transfer. Regardless of the procedure, a patient undertakes, rapid revascularization of damaged nerves or grafts is mandatory to maintain or restore viable Schwann cells and to improve the rate and quality of nerve regeneration (Bunge, 1994; Best et al., 1999; Mompeo et al., 2003; Kannan et al., 2005; Sekiguchi et al., 2012).

NO is a crucial signaling molecule associated with several physiological processes, including angiogenesis, inhibition of thrombus formation, wound healing, and neurotransmission; therefore, several studies have focused on NO-based therapies (Carpenter and Schoenfisch, 2012; Riccio and Schoenfisch, 2012; Seabra et al., 2015). Low-molecular-weight NO donors, including sodium nitroprusside (Seabra et al., 2015), nitroglycerin, NO-aspirin (Song et al., 2018), S-nitrosothiols (Seabra et al., 2004), organic nitrates (Riccio and Schoenfisch, 2012), and N-diazeniumdiolates (Keefer, 2011) have been developed for the chemical storage and delivery of NO. However, these NO donors have some disadvantages

as therapeutic tools, such as untargeted delivery, evolving tolerance for some drugs, toxicity, limited NO payload, and uncontrolled NO release (Carpenter and Schoenfisch, 2012; Riccio and Schoenfisch, 2012; Seabra et al., 2015). Thus, previous studies on NO-based therapies have mainly focused on the synthesis of controlled and sustained NO-releasing materials, and these materials have now been widely applied in biomedical fields, including cardiovascular devices, treatment of sexual dysfunction, wound healing, and antibacterial and antitumor treatments (Hetrick et al., 2008; Stevens et al., 2010; Seabra et al., 2004, 2015; Nichols et al., 2012). Silica-based materials have been widely used in the biomedical field, owing to their stability, excellent biocompatibility, straightforward synthesis, and easy customization of the size, morphology, and composition (Riccio and Schoenfisch, 2012). However, to the best of our knowledge, locally delivered exogenous NO stimulation, including that caused by the NO-SNs used in this study, has not been investigated in all animal models of PNI.

Our data showed that fibrin gel containing NO-SNs increased the capillary density at the crushing site of the sciatic nerve at 3 days after injury, and preserved the wet muscle weight and myelinated axons by 3 weeks of injury. We postulated that rapid revascularization stimulated by NO-SNs promoted axonal regeneration, preserved the myelin sheath, and prevented denervation-induced muscle atrophy in the early stages, which resulted in significantly higher SFI from 2 to 4 weeks after the injury in the group treated with NO-SNs. Blood supply is critically important for restoring or maintaining Schwann cells, influencing their activity, and promoting successful nerve regeneration (Bunge, 1994; Best et al., 1999; Mompeo et al., 2003; Kannan et al., 2005; Sekiguchi et al., 2012). However, there is a discrepancy between the beneficial effects of NO and motor functional recovery. NO-SN releases the majority of NO for up to 30 hours after injury, which is a crucial time period in revascularization and Wallerian degeneration. Successful peripheral axonal regeneration is associated with rapid and efficient Wallerian degeneration. NO-SN promotes revascularization and the rapid recruitment of cells, including macrophages, and mediates Wallerian degeneration regardless of revascularization (Rudic et al., 1998; Gonzalez-Hernandez and Rustioni, 1999a, b; Keilhoff et al., 2002a, b; Kikuchi et al., 2018). We speculate that NO-SN treatment creates a favorable environment for regenerating axons for a certain duration, which does not contribute to functional recovery. After a certain time period, axons regenerate to the end-organ (muscle), which might contribute to functional recovery.

Unlike functional improvement in the early phase, there was no difference in the number of myelinated axons and wet muscle weight at 6 weeks after injury, or SFI at 5 and 6 weeks after injury in both groups. We speculate that rapid revascularization stimulated by NO-SNs may have little influence on long-term functional outcomes after nerve damage. Similar observations have been reported by other investigators (Kelihoff et al., 2002b; Giusti et al., 2016; Lee et al., 2016). Vascular endothelial growth factor promotes early revascularization of nerve grafts, but does not improve functional motor recovery in the long term (Giusti et al., 2016; Lee et al., 2016). Although revascularization was delayed after nerve transection in eNOS KO mice, functional recovery of eNOS KO mice was similar to that in wild-type mice (Kelihoff et al., 2002b). However, our data showed that fibrin gel containing NO-SNs improved the TA contraction force at 6 weeks after injury, despite the similar number of myelinated axons and muscle weight at 6 weeks after injury in both groups. This can be explained by the fact that NO is required for the reconnection and maturation of the neuromuscular junction (Sunico et al., 2005). It is possible that the ability of the rats to undergo high and rapid intrinsic nerve regeneration (Kaplan et al., 2015) made the effect of NO less effective. Therefore, further investigations with animal models of low intrinsic recovery levels (e.g. medium/large animal models (Wang et al., 2005) or rat models using allograft (Amniattalab and Mohammadi, 2017), xenograft (Hebebrand et al., 1997), or artificial materials (Zhou et al., 2017)) are necessary to determine the possible effects and benefits of NO-releasing nanomaterials in long-term functional recovery.

The limitation of this study is that the control group should have been treated with fibrin gels containing silica nanoparticles for a stricter comparison, although it is widely accepted that mesoporous silica nanoparticles are biocompatible (Stein et al., 2000; Sayari et al., 2001; Jafari et al., 2019). SFI should have been measured from the same cohort of rats until 6 weeks, i.e. 10 rats per group after excluding 10 sacrificed rats at 3 weeks. In addition, the NO concentration (70 μM) was drawn from previous *in vitro* results (Jeon et al., 2019) multiplied by an arbitrary factor. However, for precise NO dose control, the diffusion length of NO in the gel (~100 μm from the source (Wang et al., 2017)) should be quantitatively considered. Recent developments in spatially controlled NO delivery (Park et al., 2020) would enable the quantitative study of the optimized dose of NO in nerve regeneration.

Conclusion

Our results suggest that NO-SNs (MAP3/NO) enhance the revascularization of rat sciatic nerves in the early stages after crushing injury. Exogenous nitric oxide delivered by nanomaterials enhanced axonal regeneration and functional recovery in the early phase, as supported by morphometric analysis and sciatic functional assessment. Based on our findings, we suggest a practical method to therapeutically use exogenous nitric oxide. Future studies will focus on determining the optimal dose of NO-SNs using animal models with low intrinsic recovery levels to confirm the benefits of NO-SNs in promoting revascularization for peripheral nerve regeneration.

Author contributions: *Investigation, Methodology, in vivo operation, Formal analysis, Validation, Data curation, Visualization, Writing - original draft, Writing – review & editing, Funding acquisition: JIL. Investigation, Methodology, in vivo operation, Formal analysis, Validation, Data curation, Visualization, Writing – original draft, Writing – review & editing: JHP. Synthesis and validation of NO-SNs and Writing – methods: YRK. Synthesis and validation of NO-SNs, Writing – methods: KG. Investigation, Methodology, in vivo assistance, Writing – methods, Visualization (Scheme): HWH. Investigation, Methodology, in vivo assistance, Writing – confirmation of methods: GJ. Conceptualization, Methodology: JYL. Methodology and Supervision: JYS. Conceptualization, Supervision, Writing – review and editing, Funding acquisition: JWP and JHS. Conceptualization, in vivo assistance, Supervision, Writing – major editing of original draft, Funding acquisition: MRO. All authors reviewed and approved the final draft of the manuscript.*
Conflicts of interest: *The authors have no conflicts of interest to declare.*
Availability of data and materials: *All data generated or analyzed during this study are included in this published article and its supplementary information files.*

References

Amniattalab A, Mohammadi R (2017) Functional, histopathological and immunohistichemical assessments of cyclosporine A on sciatic nerve regeneration using allografts: a rat sciatic nerve model. Bull Emerg Trauma 5:152-159.

Bain JR, Mackinnon SE, Hunter DA (1989) Functional evaluation of complete sciatic, peroneal, and posterior tibial nerve lesions in the rat. Plast Reconstr Surg 83:129-138.

Bergmeister KD, Große-Hartlage L, Daeschler SC, Rhodius P, Böcker A, Beyersdorff M, Kern AO, Kneser U, Harhaus L (2020) Acute and long-term costs of 268 peripheral nerve injuries in the upper extremity. PLoS One 15:e0229530.

Best TJ, Mackinnon SE, Midha R, Hunter DA, Evans PJ (1999) Revascularization of peripheral nerve autografts and allografts. Plast Reconstr Surg 104:152-160.

Bunge RP (1994) The role of the Schwann cell in trophic support and regeneration. J Neurol 24:S19-21.

Carpenter AW, Schoenfisch MH (2012) Nitric oxide release: part II. Therapeutic applications. Chem Soc Rev 41:3742-3752.

Chan KM, Gordon T, Zochodne DW, Power HA (2014) Improving peripheral nerve regeneration: from molecular mechanisms to potential therapeutic targets. Exp Neurol 261:826-835.

Elfar JC, Jacobson JA, Puzas JE, Rosier RN, Zuscik MJ (2008) Erythropoietin accelerates functional recovery after peripheral nerve injury. J Bone Joint Surg Am 90:1644-1653.

Geary MB, Li H, Zingman A, Ketz J, Zuscik M, De Mesy Bentley KL, Noble M, Elfar JC (2017) Erythropoietin accelerates functional recovery after moderate sciatic nerve crush injury. Muscle Nerve 56:143-151.

Giusti G, Lee JY, Kremer T, Friedrich P, Bishop AT, Shin AY (2016) The influence of vascularization of transplanted processed allograft nerve on return of motor function in rats. Microsurg 36:134-143.

Gonzalez-Hernandez T, Rustioni A (1999a) Expression of three forms of nitric oxide synthase in peripheral nerve regeneration. J Neurosci Res 55:198-207.

Gonzalez-Hernandez T, Rustioni A (1999b) Nitric oxide synthase and growth-associated protein are coexpressed in primary sensory neurons after peripheral injury. J Comp Neurol 404:64-74.

Hebebrand D, Zohman G, Jones NF (1997) Nerve xenograft transplantation. Immunosuppression with FK-506 and RS-61443. J Hand Surg Br 22:304-307.

Hetrick EM, Shin JH, Stasko NA, Johnson CB, Wespe DA, Holmuhamedov E, Schoenfisch MH (2008) Bactericidal efficacy of nitric oxide-releasing silica nanoparticles. ACS Nano 2:235-246.

Hetrick EM, Shin JH, Paul HS, Schoenfisch MH (2009) Anti-biofilm efficacy of nitric oxide-releasing silica nanoparticles. Biomaterials 30:2782-2789.

Jafari A, Derakhshankhah H, Alaei L, Fattahi A, Varnamkhasti BS, Saboury AA (2019) Mesoporous silica nanoparticles for therapeutic/diagnostic applications. Biomed Pharm 109:1100-1111.

Jeon JK, Seo H, Park J, Son SJ, Kim YR, Kim ES, Park JW, Jung WG, Jeon H, Kim YC, Seok HK, Shin JH, Ok MR (2019) Conceptual study for tissue-regenerative biodegradable magnesium implant integrated with nitric oxide-releasing nanofibers. Met Mater Int 25:1098-1107.

Kannan RY, Salacinski HJ, Sales K, Butler P, Seifalian AM (2005) The roles of tissue engineering and vascularisation in the development of micro-vascular networks: a review. Biomaterials 26:1857-1875.

Kaplan HM, Mishra P, Kohn J (2015) The overwhelming use of rat models in nerve regeneration research may compromise designs of nerve guidence conduits for humans. J Mater Sci Mater Med 26:226.

Keefer LK (2011) Fifty years of diazeniumdiolate research. From laboratory curiosity to broad-spectrum biomedical advances. ACS Chem Biol 6:1147-1155.

Keilhoff G, Fansa H, Wolf G (2002a) Differences in peripheral nerve degeneration/regeneration between wild-type and neuronal nitric oxide synthase knockout mice. J Neurosci Res 68:432-441.

Keilhoff G, Wolf G, Fansa H (2002b) NOS-mediated differences in peripheral nerve graft revascularization and regeneration. Neuroreport 13:1463-1468.

Kikuchi R, Ambe K, Kon H, Takada S, Watanabe H (2018) Nitric oxide synthase (NOS) isoform expression after peripheral nerve transection in mice. Bull Tokyo Dent Coll 59:15-25.

Lee JI, Nha KW, Suh JS, Choo SK, Park JH, Park JW (2013) Remote postconditioning attenuates ischemia/reperfusion injury in rat skeletal muscle through mitochondrial ATP-sensitive K+ channel-dependent mechanism. J Reconstr Microsurg 29:571-578.

Lee JI, Hur JM, You J, Lee DH (2020) Functional recovery with histomorphometric analysis of nerves and muscles after combination treatment with erythropoietin and dexamethasone in acute peripheral nerve injury. PLoS One 15:e0238208.

Lee JY, Giusti G, Friedrich PF, Bishop AT, Shin AY (2016) Effect of vascular endothelial growth factor administration on nerve regeneration after autologous nerve grafting. J Reconstr Microsurg 32:183-188.

Levy D, Kubes P, Zochodne DW (2001) Delayed peripheral nerve degeneration, regeneration, and pain in mice lacking inducible nitric oxide synthase. J Neuropathol Exp Neurol 60:411-421.

Mompeo B, Engele J, Spanel-Borowski K (2003) Endothelial cell influence on dorsal root ganglion cell formation. J Neurocytol 32:123-129.

Moreno-Lopez B (2010) Local isoform-specific NOS inhibition: a promising approach to promote motor function recovery after nerve injury. J Neurosci Res 88:1846-1857.

Nichols SP, Storm WL, Koh A, Schoenfisch MH (2012) Local delivery of nitric oxide: targeted delivery of therapeutics to bone and connective tissues. Adv Drug Deliv Rev 64:1177-1188.

Noori A, Ashrafi SJ, Vaez-Ghaemi R, Hatamian-Zaremi A, Webster TJ (2017) A review of fibrin and fibrin composites for bone tissue engineering. Int J Nanomed 12:4937-4961.

Park J, Jin K, Sahasrabudhe A, Chiang PH, Maalouf JH, Koehler F, Rosenfeld D, Rao S, Tanaka T, Khudiyev T, Schiffer ZJ, Fink Y, Yizhar O, Manthiram K, Anikeeva P (2020) In situ electrochemical generation of nitric oxide for neuronal modulation. Nat Nanotechnol 15:690-697.

Percie du Sert N, Ahluwalia A, Alam S, Avey MT, Baker M, Browne WJ, Clark A, Cuthill IC, Dirnagl U, Emerson M, Garner P, Holgate ST, Howells DW, Hurst V, Karp NA, Lazic SE, Lidster K, MacCallum CJ, Macleod M, Pearl EJ, et al. (2020) Reporting animal research: Explanation and elaboration for the ARRIVE guidelines 2.0. PLoS Biol 18:e3000411.

Riccio DA, Schoenfisch MH (2012) Nitric oxide release: part I. Macromolecular scaffolds. Chem Soc Rev 41:3731-3741.

Rudic RD, Shesely EG, Maeda N, Smithies O, Segal SS, Sessa WC (1998) Direct evidence for the importance of endothelium-derived nitric oxide in vascular remodeling. J Clin Invest 101:731-736.

Sayari A, Hamoudi S (2001) Periodic mesoporous silica-based organic-inorganic nanocomposite materials. Chem Mater 13:3151-3168.

Seabra AB, Fitzpatrick A, Paul J, De Oliveira MG, Weller R (2004) Topically applied S-nitrosothiol-containing hydrogels as experimental and pharmacological nitric oxide donors in human skin. Br J Dermatol 151:977-983.

Seabra AB, Justo GZ, Haddad PS (2015) State of the art, challenges and perspectives in the design of nitric oxide-releasing polymeric nanomaterials for biomedical applications. Biotechnol Adv 33:1370-1379.

Sekiguchi H, Ii M, Jujo K, Renault MA, Thorne T, Clarke T, Ito A, Tanaka T, Klyachko E, Tabata Y, Hagiwara N, Losordo D (2012) Estradiol triggers sonic-hedgehog-induced angiogenesis during peripheral nerve regeneration by downregulating hedgehog-interacting protein. Lab Invest 92:532-542.

Shin JH, Metzger SK, Schoenfisch MH (2007) Synthesis of nitric oxide-releasing silica nanoparticles. J Am Chem Soc 129:4612-4619.

Shin JH, Schoenfisch MH (2008) Inorganic/organic hybrid silica nanoparticles as a nitric oxide delivery scaffold. Chem Mater 20:239-249.

Song JM, Upadhyaya P, Kassie F (2018) Nitric oxide-donating aspirin (NO-Aspirin) suppresses lung tumorigenesis in vitro and in-vivo and these effects are associated with modulation of the EGFR signaling pathway. Carcinogenesis 39:911-920.

Stein A, Melde BJ, Schroden RC (2000) Hybrid inorganic-organic mesoporous silicates—nanoscopic reactors coming of age. Adv Mater 12:1403-1419.

Stevens EV, Carpenter AW, Shin JH, Liu J, Der CJ, Schoenfisch MH (2010) Nitric oxide-releasing silica nanoparticle inhibition of ovarian cancer cell growth. Mol Pharm 7:775-785.

Sundem L, Chris Tseng KC, Li H, Ketz J, Noble M, Elfar J (2016) Erythropoietin enhanced recovery after traumatic nerve injury: myelination and localized effects. J Hand Surg 41:999-1010.

Sunico CR, Portillo F, Gonzalez-Forero D, Moreno-Lopez B (2005) Nitric-oxide-directed synaptic remodeling in the adult mammal CNS. J Neurosci 25:1448-1458.

Tapp M, Wenzinger E, Tarabishy S, Ricci J, Herrera FA (2019) The epidemiology of upper extremity nerve injuries and associated cost in the US emergency departments. Ann Plast Surg 83:676-680.

Tobin CA, Wang Z, Zhang LL, Agresti M, Grewal P, Matloub HS, Yan JG (2014) A new computerized morphometric analysis for peripheral nerve study. J Reconstr Microsurg 30:75-82.

Wang X, Hu W, Cao Y, Yao J, Wu J, Gu X (2005) Dog sciatic nerve regeneration across a 30-mm defect bridged by a chitosan/PGA artificial nerve graft. Brain 128:1897-1910.

Wang Z, Wen F, Zhang R, Zhang Q (2017) Modulated nitric oxide delivery in three-dimensional biomaterials for vascular functionality. MRS Comm 7:348-360.

Zhou C, Liu B, Huang Y, Zeng X, You H, Li J, Zhang Y (2017) The effect of four types of artificial nervegraft structures on the repair of 10-mm rat sciatic nerve gap. J Biomed Mater Res Part A 105A:3077-3085.

Zochodne DW, Levy D (2005) Nitric oxide in damage, disease and repair of the peripheral nervous system. Cell Mol Biol 51:255-267.

C-Editors: Zhao M, Li CH; T-Editor: Jia Y